International Journal of Applied Science and Engineering
2006. 4, 2: 127-150

Application of Closed-Form Solution for Normal Surface Displacements on Impacted Half Space : Quantification of Impact-Echo Signals

Chih-Peng Yu *, Chia-Chi Cheng, and Jiunnren Lai

Department of Construction Engineering,
Chaoyang University of Technology, Wufeng 413, Taiwan (R.O.C.)

Abstract: In order to investigate the feasibility of deducing a simulated transfer function based on the Rayleigh wave form in an Impact-Echo signal, the analytical solution for the normal surface displacement due to a heaviside force at the half-space was reviewed and used to compute the surface displacement responses resulted from various types of impulse forces. Based on a series of numerical studies on the characteristics of Rayleigh wave form in the surface displacement responses, this paper presents the idea of using an equivalent impact force to derive an intentionally scaled transfer function. The pseudo force can be obtained from using Rayleigh wave form as a pseudo force or by generating an equivalent half-sine impact force accordingly. The effect of using such pseudo and equivalent force functions was discussed in details. In the proposed method, the force amplitude was first estimated from an amplitude curve established from numerical simulations using half-sine force functions. The recovery of a simulated transfer function was next achieved via the use of an estimated force amplitude and a selected force function. The proposed procedure also results in steady thickness amplitudes when measurements on two concrete plates were taken for various impacts associated with different steel balls and different impact locations. The success in recovering constant thickness amplitudes for plate-like structural members proved that the derivation of simulated transfer function is a useful tool in extending the Impact-Echo test. The quantitative evaluation of the interfacial property of the substrate layer will also benefit from this simulated transfer function.

Keywords: Impact-Echo, transfer function, Rayleigh wave form, normal response on a half-space

1. Introduction

The use of an impact-type force as the energy source of stress waves has been adopted in many NDT methods, such as the well-known Impact-Echo method, Sonic Echo/Impulse Response method, and Spectral Analysis of Surface Waves (SASW) method. Some of these NDT methods consist of analysis procedures in the frequency domain, and thus, either the frequency amplitude spectrum or the transfer function is computed for the recorded responses.

For methods involving analysis of amplitude spectra, for example Impact-Echo method, the frequency of the dominant peak shown in an amplitude spectrum normally provides the thickness information of the specimen. Thus,

* Corresponding author; e-mail: cpyu@mail.cyut.edu.tw
Accepted for Publication: July 28, 2006

in an Impact-Echo analysis, it is often called thickness frequency. Since the amplitude changes with magnitude and duration of the impact, the amplitude itself fails to provide further information, namely the characteristics of the interface. Clearly, amplitudes recorded in different tests cannot be compared with each other unless the force functions are given. In order to distinguish between various reflected interfaces, it is necessary to normalize frequency spectra by an equivalent force function so that the thickness amplitude associated with a free surface at bottom remains constant for a given specimen.

When a concrete plate is placed on a material of smaller acoustic impedance such as soil, epoxy, and wood, the thickness frequency of the plate is the same as the one reflected free on bottom surface. However, the amplitude should be lower since stress waves are also propagated into the substrate layer. Accordingly, the material property under the concrete plate could be quantitatively evaluated from the thickness amplitude. Furthermore, the debonded or partially debonded condition between concrete and substrate material might also be identified. In other words, transfer functions are preferable when dealing with the identification of substrate layers.

In a traditional Impact-Echo test, the force function is not recorded. In order to recover the force function due to an impact-type force, we first review the explicit solution by Pekeris [1]. His solution for the surface responses due to a concentrated force applying on the surface of a semi-infinite medium is derived based on a fixed Poisson's ratio of 0.25. We will extend the solution formulation for the normal response to account for an arbitrary Poisson's ratio. Next, we will summarize the fundamental characteristics of normal surface responses obtained numerically for various types of force functions and for materials with different Poisson's ratios. A procedure to reproduce a simulated transfer function, proven to be beneficiary to the Impact-Echo analysis, will be proposed in the end.

2. Theoretical background

Regarding the impact response on a semi-infinite medium, the analytical solution can normally be derived in time domain through the convolution of force functions with the Green function or in frequency domain by inversely transforming the product between frequency contents of the force functions and the transfer function. However, when the response due to heaviside step function is given, an alternative approach is to numerically evaluate solutions by the method of superposition. Procedures using the integral transform technique to derive the analytical solution of the surface response due to heaviside step force were first proposed by Pekeris [1] and can be found in several textbooks, such as Achenbach [2] and Graff [3]. It is shown in Equation (1) the solution form of the problem. The normal surface displacement is expressed as the function of a dimensionless time parameter, τ, the relative ratio of the elapsed time to the arrival time of shear wave. The time history of responses can be obtained by numerically computing the two integral terms.

$$u_z(r,0,t)=\begin{cases}0 & ,\tau\le\sigma\\ \dfrac{Z}{\pi^2\mu r}F_1(\tau) & ,\sigma\le\tau\le 1\\ \dfrac{Z}{\pi^2\mu r}\left[F_1(1)+F_2(\tau)\right] & ,\tau>1\end{cases} \tag{1}$$

where the two functions have the integral forms as

$$F_1(\tau)=\int_\sigma^\tau \frac{y\sqrt{y^2-\sigma^2}(1-2y^2)^2}{\sqrt{\tau^2-y^2}R(y)}dy$$

$$F_2(\tau)=\mathbf{P}\int_1^\tau \frac{y\sqrt{y^2-\sigma^2}}{\sqrt{\tau^2-y^2}R(y)}\,dy$$

with σ the ratio of shear wave velocity to longitudinal wave velocity, $R(y)$ the charac-

teristic Equation of the Rayleigh wave and the symbol **P** representing the principal-value of the integral.

Pekeris [1] shows that, by change of variables, the integral solutions in Equation (1) can be further reduced to an algebraic form of simpler rational functions. The result is the solution for the special case ν = 0.25 and is given as Equation (2).

$$u_z(r,0,t) = w(t) =$$

$$\begin{cases} 0, & \tau < 1/\sqrt{3} \\ -\dfrac{Z}{32\mu\pi r}\left\{6-\left(\dfrac{3}{\tau^2-\frac{1}{4}}\right)^{\frac{1}{2}}-\left(\dfrac{3\sqrt{3}+5}{\frac{3}{4}+\frac{\sqrt{3}}{4}-\tau^2}\right)^{\frac{1}{2}}+\left(\dfrac{3\sqrt{3}-5}{\tau^2+\frac{\sqrt{3}}{4}-\frac{3}{4}}\right)^{\frac{1}{2}}\right\}, & 1/\sqrt{3} < \tau < 1 \\ -\dfrac{Z}{16\pi\mu r}\left\{6-\left(\dfrac{3\sqrt{3}+5}{\frac{3}{4}+\frac{\sqrt{3}}{4}-\tau^2}\right)^{\frac{1}{2}}\right\}, & 1 < \tau < \gamma \\ -\dfrac{3Z}{8\pi\mu r}, & \tau > \gamma, \end{cases} \tag{2}$$

with
r is radial distance
μ is Lame's elastic constant = G (shear modulus)
Z is the amplitude of the Heaviside step force
t is time
ρ is mass density

$$\gamma = \frac{(3+\sqrt{3})^{\frac{1}{2}}}{2}$$

$$\tau = \frac{C_S t}{r}$$

$$C_s = \sqrt{\frac{\mu}{\rho}}$$

Although Equation (1) can be numerically evaluated without difficulty, an explicit type solution like Equation (2) is more straight forward and may be able to provide a quantitative reference for the Rayleigh wave (R-wave) responses. In Equation (2), the solution is separated into four parts by τ being equal to $1/\sqrt{3}$, 1 and γ. These three values of τ stand for the first arrivals of P-wave, S-wave, and R-wave, respectively. It is interesting to note that the solution exhibits a singular point at τ = γ .which results in the R-wave dominated phenomenon. As a result, the R-wave portion of the surface response is of particular importance in problems associated with surface responses.

Following the solution procedure proposed by Pekeris and keeping Poisson's ratio, ν, as a variable in the derivation, a general solution valid for all Poisson's ratios can be obtained in Pekeris' original format as follows.

$$\begin{cases} w(\tau) = 0 \quad , \ \tau < \sigma \\ w(\tau) = \dfrac{Z}{32\pi\mu r(\sigma^2-1)}\,\mathrm{Re}\left\{4-\dfrac{\bar{A}}{(\tau^2-a)^{1/2}}-\dfrac{\bar{B}}{(\tau^2-b)^{1/2}}-\dfrac{\bar{C}}{(c-\tau^2)^{1/2}}\right\} \ , \sigma < \tau < 1 \\ w(\tau) = \dfrac{Z}{16\pi\mu r(\sigma^2-1)}\left\{4-\dfrac{\bar{C}}{(c-\tau^2)^{1/2}}\right\} \quad , 1 < \tau < \sqrt{c} \\ w(\tau) = \dfrac{Z}{4\pi\mu r(\sigma^2-1)} = ZA_0(r,\mu,\nu) \quad , \tau > \sqrt{c} \end{cases} \tag{3}$$

in which a, b and c are the three roots of y^2 in Equation (4).

$$R(y) = (2y^2-1)^2 - 4y^2(y^2-\sigma^2)^{1/2}(y^2-1)^{1/2}$$
$$= 16(\sigma^2-1)y^6 + 8(3-2\sigma^2)y^4 - 8y^2 + 1 \quad (4)$$
$$= (y^2-a)(y^2-b)(y^2-c)$$

with $y = C_s/C_R$ and $\sigma = C_s/C_p = \sqrt{(1-2\nu)/2(1-\nu)}$. C_p, C_s and C_R are the wave velocities of the P-wave, S-wave and R-wave, respectively. Equation (4) is the characteristic Equation of the Rayleigh surface wave with a and c being denoted the smallest and largest of the three roots of $R(y^2) = 0$. In addition, A_0 is the steady-state displacement due to heaviside step force and can be defined as a nominal amplitude factor to quantify displacement amplitude caused by impulse-type forces.

Equation (4) indicates that when $\nu \leq 0.263$, we have $a < b < \sigma^2 < 1 < c$ with a, b, and c all real numbers. On the other hand, when $\nu > 0.263$, a and b become a pair of conjugate complex numbers and we have $\mathrm{Re}(a) = \mathrm{Re}(b) < \sigma^2 < 1 < c$. The remaining three coefficients in the numerators, $\bar{A}$, $\bar{B}$, and $\bar{C}$, are functions of a, b, c, and σ^2 as shown in Equation (5).

$$\bar{A} = \frac{4a(1-a)^{1/2}(\sigma^2-a)}{(a-b)(a-c)} = \frac{(2a-1)^2(\sigma^2-a)^{1/2}}{(a-b)(a-c)}$$
$$\bar{B} = \frac{4b(1-b)^{1/2}(\sigma^2-b)}{(b-c)(b-a)} \quad (5)$$
$$\bar{C} = \frac{4c(c-1)^{1/2}(c-\sigma^2)}{(c-a)(c-b)}$$

When the Poisson's ratio is 0.25, the three roots of Equation (4) are $a = \frac{1}{4}$, $b = \frac{3-\sqrt{3}}{4}$, $c = \frac{3+\sqrt{3}}{4}$ and the constant σ^2 equals 1/3. Substitution of these values into Equation (5) gives $\bar{A} = \frac{2}{\sqrt{3}}$, $\bar{B} = -\frac{2\sqrt{3\sqrt{3}-5}}{3}$, $\bar{C} = \frac{2\sqrt{3\sqrt{3}-5}}{3}$, and $A_0 = \frac{-3}{8\pi\mu r}$. Thus, Equation (3) is reduced to Equation (2). Figure 1 concludes the dimensionless displacement responses associated with five Poisson's ratios, 0.1, 0.18, 0.25, 0.33, and 0.4 .

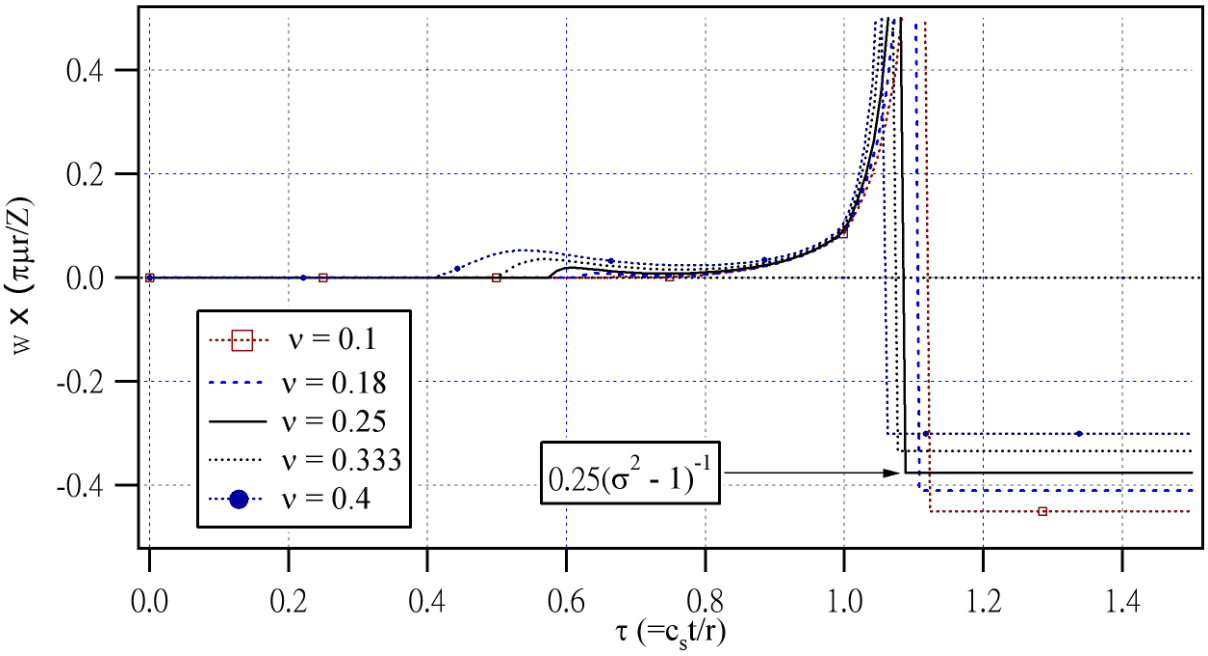

Figuer 1. Vertical displacement at free surface according to Equation (3)

For a given force-time function, $f(t)$, the corresponding vertical displacement at the free surface $W(t)$ can be computed by employing the method of superposition as shown in Wu et al. [4]. In their work, the force-time function is first discretized into n segments and expressed as the summation of n+1 heaviside functions, $H(t)$, as shown in Equation (6).

$$f(t) = \sum_{k=0}^{n} a_k H(t - k\Delta t) \tag{6}$$

Then the surface response with respect to any arbitrary force–time function can be evaluated from summing up contributions from all heaviside functions as Equation (7).

$$W(t) = \sum_{k=0}^{n} a_k w(\tau - k\Delta\tau) \tag{7}$$

where $w(\ )$ is shown in Equation (3) and the dimensionless time variable $\tau = tC_s/r$.

3. Numerical simulations of impact responses

In the following, the characteristics of impacted surface responses due to different impact force functions are discussed. Figure 2 shows the typical surface response due to an impact force, in which A_t and A_{peak} denote the amplitudes associated with the trough prior to the R-wave arrival and the compressive (positive) peak of the R-wave signal, respectively. To estimate the duration of the impact, two durations τ_d and τ_0 are defined in which the former represents the elapsed time between trough and ending of the R-wave signal, and the latter stands for the duration of the entire compressive response between two zero crossings.

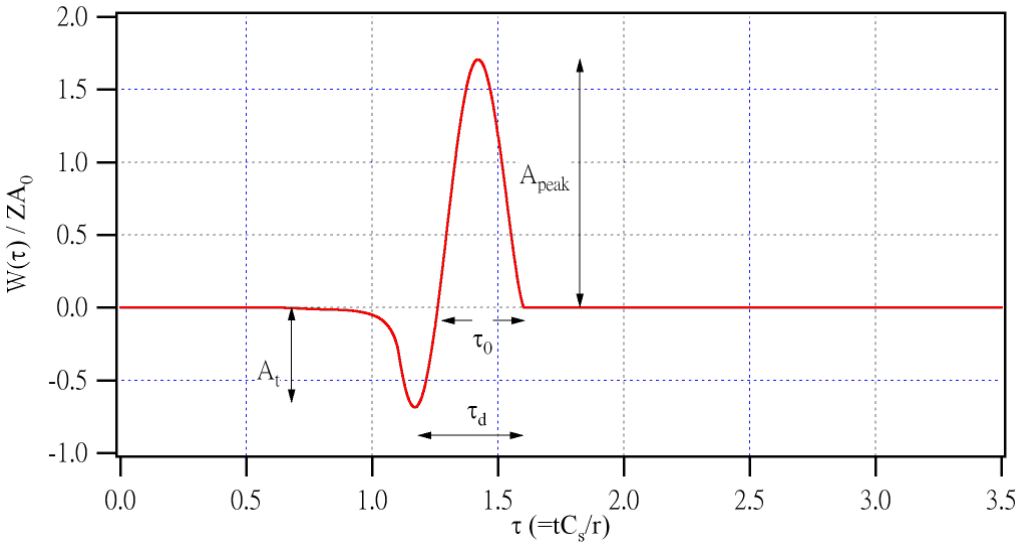

Figure 2. A typical surface displacement response due to an impact force

Figure 3 shows the surface responses corresponding to various types of impact forces in which impact durations for all forces are the same, $\tau_D = 2$. In Figure 3(a), responses due to a half-sine function, a triangle function, and an impulse function obtained from matching the shape of the force function with that of an arbitrarily selected impact created by hitting a concrete surface with a PCB 086C03 hammer. It is clear that the trough-to-ending duration, τ_d, associated with the half-sine and the triangle functions equal to the impact duration τ_D

since the arrival and ending time of the impact forces can be easily recognized by the abrupt changes of curves. On the other hand, a more realistic force function, denoted as "hammer" in the Figure, leads to a smoother trough in the response curve and thus relatively smaller values for τ_d. The reason why response curves show abrupt changes at trough and ending points is that the slopes at the beginning and the ending of the force functions are not continuous. In Figure 3(c), responses curves due to half-sine-squared and half-sin$^{1.5}$ are compared with that of half-sine. Because the slopes at the starting and ending points of the sin^2 and sin$^{1.5}$ functions are continuous, their corresponding response curves appear to have smoother troughs as that shown in the realistic case.

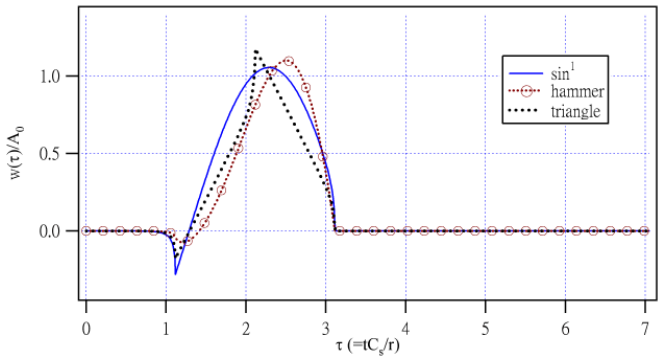

(a) surface responses w.r.t. impact forces in (b)

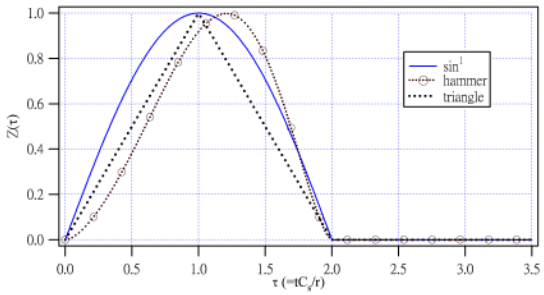

(b) force functions

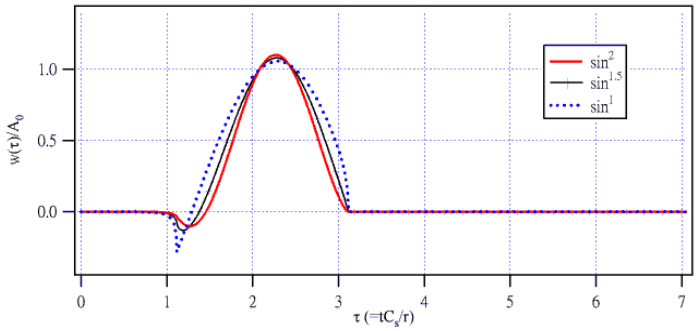

(c) surface responses w.r.t. impact forces in (d)

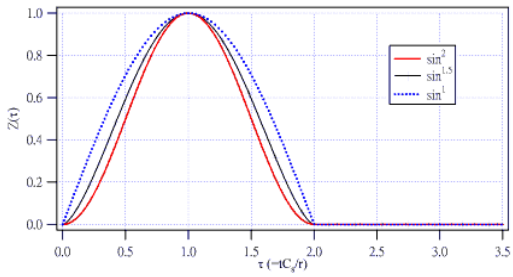

(d) half-sine-powered force functions

Figure 3. Surface responses due to various types of force functions for $\tau_D = 2$ and $\nu = 0.18$

The trough-to-ending duration, τ_d, the compressive duration, τ_0, the peak amplitude, A_{peak}, and the trough amplitude, A_t, associated with various force functions are summarized in Table 1. It can be seen from Table 1 that the realistic case is close to and falls between the half-sine-squared and half-sin$^{1.5}$ cases. As far as the amplitudes A_{peak} and A_t are concerned, the half-sine-squared force function seems an appropriate approximation for the realistic impulse that we arbitrarily selected for this work. Therefore, the half-sine-squared function is also selected to illustrate the variation of duration differences with the size of impact duration τ_D, as shown in Table 2.

Table 1. Comparisons between responses due to various force functions ($\tau_D = 2$, $\nu = 0.18$)

Force function	τ_d	τ_0	A_{peak}	A_t	A_t / A_{peak}
Triangle	2	1.841	1.159	-0.159	0.137
Half-sine	2	1.848	1.046	-0.247	0.236
Half-sin$^{1.5}$	1.939	1.766	1.066	-0.112	0.105
Half-sine-squared	1.864	1.692	1.084	-0.084	0.078
Realistic(hammer)	1.918	1.732	1.083	-0.063	0.058

Table 2. Variation of various ratios with impact duration τ_D (half-sine-squared force, $\nu = 0.18$)

Impact duration	τ_d / τ_D	τ_0 / τ_D	τ_0 / τ_d	A_t / A_{peak}
$\tau_D = 10$	0.984	0.965	0.98	0.004
$\tau_D = 5$	0.961	0.931	0.969	0.015
$\tau_D = 2$	0.932	0.846	0.908	0.078
$\tau_D = 1$	0.899	0.764	0.850	0.203
$\tau_D = 0.5$	0.879	0.703	0.800	0.372
$\tau_D = 0.2$	0.878	0.673	0.767	0.532
$\tau_D = 0.1$	0.878	0.673	0.767	0.560

To establish the relations between impact duration τ_D and response amplitudes A_{peak} and A_t, responses due to half-sine-squared impacts of different durations are plotted in Figure 4. From Figure 4(a), it can be observed that as impact duration increases, the peak amplitude A_{peak} approaches A_0, while the trough amplitude A_t becomes less significant. For example, the ratios of A_t to A_{peak} are 0.203, 0.372 and 0.532 for impact duration τ_D equal to 1, 0.5 and 0.2, respectively. To have a better presentation of the trend of response curves, Figure 4(b) shows the variation of amplitudes with horizontal axis in logarithmic scale. The limiting amplitude ratio (A_t / A_{peak}) for very small impact duration is about 0.56 as τ_D being smaller than 0.14. Table 2 lists the duration ratios and amplitude ratios for different values of impact duration τ_D. It is interesting to note that the duration ratios appear to be fixed as the force duration becomes smaller, for instance when dimensionless duration τ_D is as small as 0.2 or less. On the other hand, when dimensionless duration τ_D is large, the trough amplitude A_t is negligible and impact duration τ_D can be roughly approximated by τ_d or τ_0.

Table 3 lists the (A_t / A_{peak}) amplitude ratios associated with different values of τ_D for various force functions. It is apparent that all force functions show similar trends regarding the variation of the (A_t / A_{peak}) ratio versus impact durations. In all cases, the ratios associated with $\tau_D = 0.1$ already equal to the limiting values obtained using very small τ_D. The realistic force function recovered from the PCB hammer gives ratios lower than those obtained from the three half-sine-powered functions. Generally speaking, the ratios by the half-sine-squared function agree with the realistic ones for large values of τ_D. For

smaller values of τ_D, results by the realistic force appear to be about 70% to 80% of those by the half-sine-squared force.

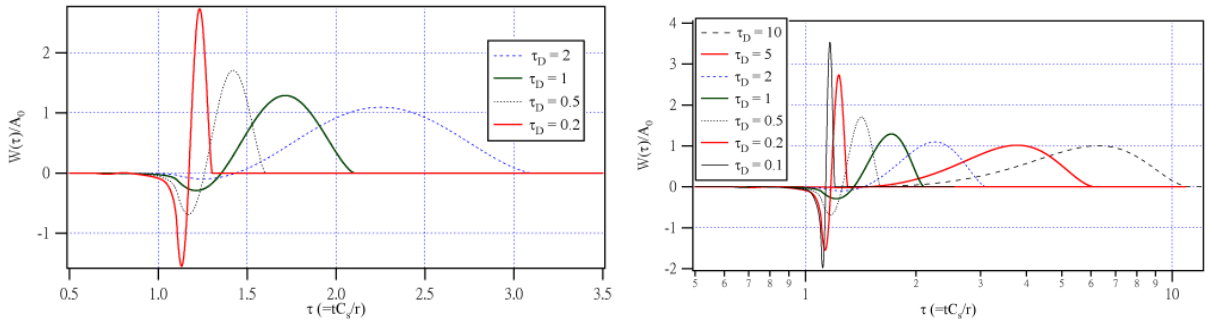

Figire 4. Surface responses due to half-sine-squared forces with $\nu = 0.18$

Table 3. Variation of amplitude ratios (A_t / A_{peak}) with impact duration τ_D ($\nu = 0.18$)

A_t / A_{peak}	sin	$\sin^{1.5}$	hammer	$\sin^2$
$\tau_D = 10$	0.050	0.010	0.005	0.004
$\tau_D = 5$	0.010	0.029	0.015	0.015
$\tau_D = 2$	0.236	0.105	0.059	0.078
$\tau_D = 1$	0.416	0.234	0.141	0.203
$\tau_D = 0.5$	0.615	0.405	0.261	0.372
$\tau_D = 0.2$	0.803	0.579	0.400	0.532
$\tau_D = 0.1$	0.864	0.620	0.440	0.560

From Figure 4(b), as impact duration τ_D increases, the peak amplitude A_{peak} shows a decreasing trend for small values of τ_D and approaches a constant, A_0, for larger values of τ_D. To have a better idea on how peak amplitude varies with impact duration, it is shown in Figure 5 the (A_{peak} / A_0) versus (τ_D) curves with half-sine force function for various Poisson's ratios. Since Figure 5 is plotted using logarithmic scales, the negative slope of minus one-half within very small values of τ_D represents that peak amplitude A_{peak} attenuates with $r^{-0.5}$. On the other hand, the peak amplitude A_{peak} equals A_0 and thus attenuates with r^{-1} for the region of larger τ_D. As shown in Figure 5, curves associated with different values of Poisson's ratios result in almost parallel lines of similar slopes for smaller τ_D and converge to a single curve for larger τ_D. To investigate the differences among (A_{peak} / A_0) versus (τ_D) curves of different force functions, Figure 6 shows the corresponding curves of four kinds of force functions for a given Poisson's ratio $\nu = 0.18$. It is shown in Figure 6 that three half-sine related curves exhibit similar trends. In addition, higher-powered sine functions appear to cause larger peak amplitudes. The triangle force function gives the highest values among all for τ_D larger than 0.5 but leads to results close to those of half-sine$^{1.5}$ for region of very small τ_D.

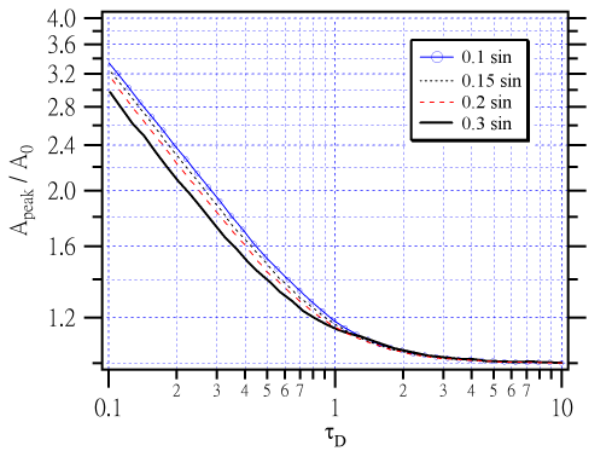

Figure 5. Amplitude ratios for half-sine curve with different Poisson's ratios

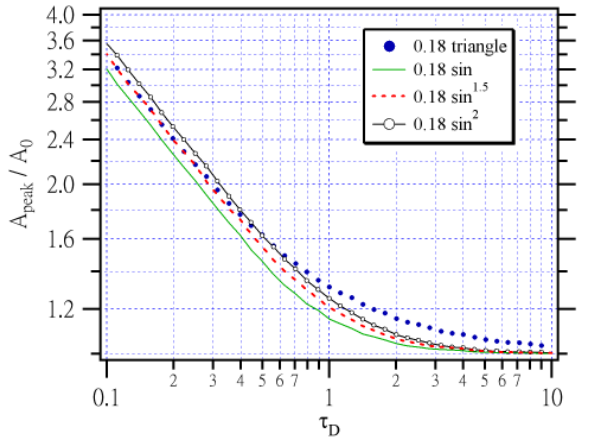

Figure 6. Amplitude ratios for different force functions with Poisson's ratio ν = 0.18

4. Recovery of impact force functions

To reasonably recover the force function of a specific surface response, one has to identify first the amplitude and the duration of the impact force. In the following, we propose a simple procedure using amplitude curves such as those shown in Figure 6 to estimate the force amplitude. Alternatively, the impact force can be simulated as an equivalent force using a relatively simple function, i.e. a half-sine function, or using a portion of the surface signal. The first approach requires an appropriate duration for the simulated force while the latter method utilizes the compressive portion of the surface response as the force function, in which the force duration is τ_0. Regarding the determination of the duration of an equivalent half-sine force, the relation between an appropriate value and the duration parameters τ_d and τ_0 is studied. It is found that such an equivalent half-sine force can reproduce similar frequency contents as those of the original impact functions and can thus provide an alternative way to compute the transfer function associated with a specific impact-echo response. Details on the determinations of force amplitude and equivalent duration of the impact are discussed as follows.

Determination of force amplitude

A realistic impact may be simulated using half-sine functions with power orders between 1.5 and 2, such as the example illustrated in Table 1. In all cases, the duration parameter τ_0 is always smaller than τ_D and the value of τ_d is ranged between τ_0 and τ_D. Using τ_d or τ_0 to represent the impact duration would under-estimate the real impact duration, τ_D. As a result, when using a smaller τ_D to establish the response amplitude A_{peak} from the half-sine$^{1.5}$ and half-sine-squared curves, higher estimates can be anticipated since A_{peak} decreases with τ_D as shown in Figure 6. On the other hand, the half-sine curve gives somehow lower values than the two higher order half-sine-powered curves. Without precise computations, using half-sine curves to establish A_{peak} may roughly balance the over-estimate caused by the designated smaller value for τ_D. The variations of the two response durations with impact duration τ_D are shown in Table 4. The corresponding predictions of amplitude ratios from the "lower" half-sine curve are shown in Table 5. To have a better look at the trends of the amplitude predictions, Figure 7 shows the predicted amplitude ratios with markers for each impact

force. According to results associated with these three cases of impact forces, it is found that the lower ratios associated with τ_d are very close to the half-sin$^{1.5}$ curve. While the higher ratios with respect to τ_0 seem basically follow the trend of the hammer curve but keep increasing as τ decreases and finally deviate from the trend. As a result, extracting amplitude ratios from the half-sine curve with durations of τ_d may provide lower bound values regardless of the types of force functions. On the other hand, the predicted values using τ_0 are higher than the true solutions, especially for smaller impact durations. However, as long as impact duration τ_D is larger than 1, the amplitude ratios predicted by half-sine agree well with the real values for all three force functions. Owing to the fact that the use of smaller response durations τ_d and τ_0 would compensate the under-estimated ratios obtained from the half-sine curve, such curve may be used to provide estimates within reasonable ranges for the amplitude ratio (A_{peak} / A_0) associated with various types of force functions.

To simplify the recovery of amplitude ratio (A_{peak} / A_0), the half-sine amplitude curve for ν = 0.18 can be approximated by three simple functions as shown in Equation (8) [5].

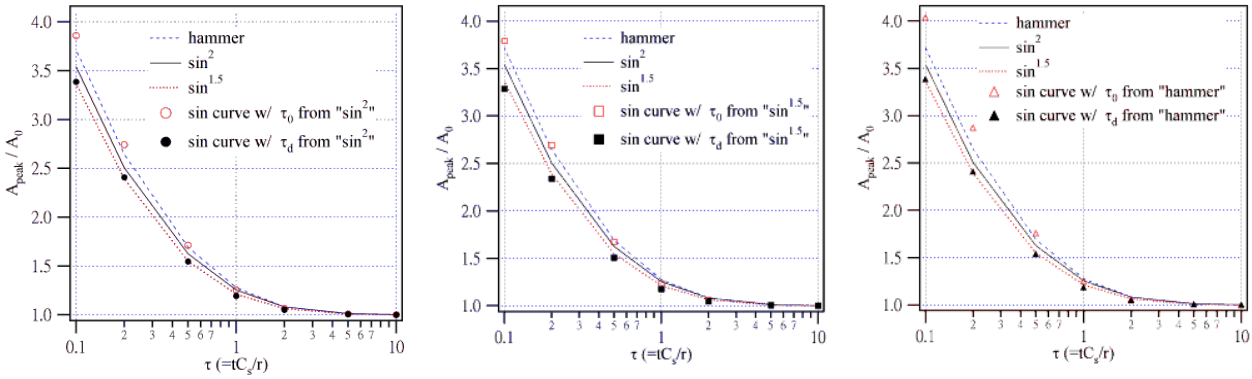

(a) predicted amplitudes w.r.t. τ_0 of half-sin^2

(b) predicted amplitudes w.r.t. τ_0 of half-sin$^{1.5}$

(c) predicted amplitudes w.r.t. τ_0 of realistic hammer record

Figure 7. Predictions of amplitude ratios using half-sine curve with τ_0 and τ_d

Table 4. Variations of τ_0 and τ_d with τ_D for half-sin^2, half-sine$^{1.5}$ and hammer forces (ν = 0.18)

	sin^2		sin$^{1.5}$		hammer	
	τ_0/τ_D	τ_d/τ_D	τ_0/τ_D	τ_d/τ_D	τ_0/τ_D	τ_d/τ_D
τ_D = 10	0.965	0.984	0.965	0.990	0.973	0.992
τ_D = 5	0.931	0.961	0.940	0.983	0.945	0.983
τ_D = 2	0.846	0.932	0.863	0.961	0.867	0.959
τ_D = 1	0.764	0.899	0.807	0.948	0.763	0.926
τ_D = 0.5	0.703	0.880	0.739	0.932	0.666	0.889
τ_D = 0.2	0.673	0.878	0.697	0.932	0.614	0.878
τ_D = 0.1	0.673	0.878	0.697	0.932	0.614	0.878

Table 5. Equivalent values of (A_{peak} / A_0) obtained from half-sine curve with τ_D replaced by τ_0 and τ_d (ν = 0.18, values associated with τ_0 and τ_d listed in Table 4)

A_{peak} / A_0	Original values			Estimates by half-sine					
	$\sin^2$	$\sin^{1.5}$	hammer	τ_0 of $\sin^2$	τ_d of $\sin^2$	τ_0 of $\sin^{1.5}$	τ_d of $\sin^{1.5}$	τ_0 of hammer	τ_d of hammer
τ_D = 10	1.004	1.003	1.002	1.002	1.002	1.002	1.002	1.002	1.002
τ_D = 5	1.015	1.011	1.012	1.009	1.008	1.009	1.008	1.008	1.008
τ_D = 2	1.084	1.066	1.083	1.064	1.053	1.061	1.050	1.061	1.050
τ_D = 1	1.256	1.213	1.278	1.254	1.195	1.233	1.177	1.254	1.186
τ_D = 0.5	1.626	1.549	1.694	1.714	1.546	1.674	1.507	1.76	1.538
τ_D = 0.2	2.505	2.392	2.646	2.744	2.408	2.692	2.338	2.871	2.408
τ_D = 0.1	3.539	3.363	3.713	3.859	3.386	3.793	3.288	4.037	3.386

$$\begin{aligned} Y &= X^{-\frac{1}{2}} && \text{for } X \le 0.4 \\ Y &= 1 + 0.12X^{-1.7} && \text{for } 0.4 \le X \le 2.5 \\ Y &= 1 && \text{for } X \ge 2.5 \end{aligned} \qquad (8)$$

in which $X = \tau_D / \sqrt{c}$, $Y = A_{peak} / A_0$, and c is defined in Equation (4).

Determination of impact duration τ_D

As shown in Table 4, the ratios of response durations (τ_0 and τ_d) to impact duration τ_D for different force functions are similar, but their differences become more significant as τ_D decreases. Figure 8 shows the variations of response durations for different force functions. It is clear that, when the anticipated value of τ_D is larger than 2, using response durations τ_d and τ_0 to predict original impact duration τ_D seems possible since differences between curves are minor. However, for cases of small τ_D, reliable predictions become relatively difficult since precise relations between the response durations and τ_D cannot be determined without prior knowledge of the force function.

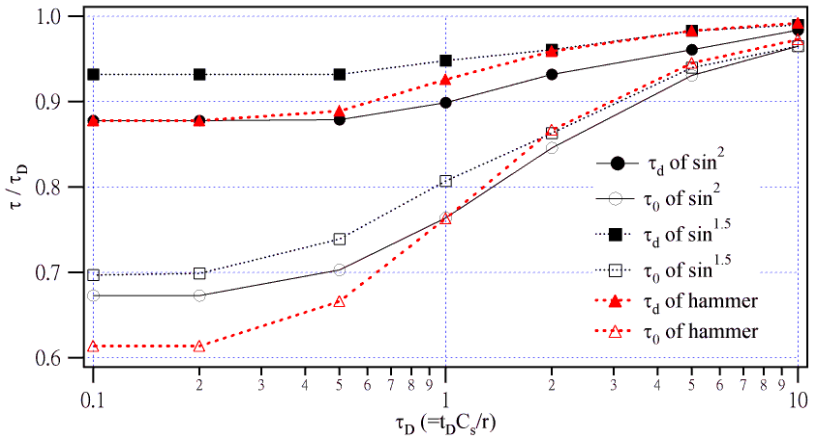

Figure 8. Variations of response durations τ_0 and τ_d with impact duration τ_D

Determination of frequency contents of impact force

In the previous two sections, we illustrate that the predictions for the amplitude and duration of an impact force can be carried out through their relations with the response durations τ_d and τ_0. Nevertheless, it is quite clear that one can not possibly recover the exact time history of force function from the established Figures and Tables. When dealing with frequency spectra, the most significant characteristics of the force function is its frequency contents. Thus, two simple approaches will be introduced to reproduce reasonable frequency contents for arbitrary force functions.

From the time history of a recorded surface response, the most straight-forward way to obtain a force function similar to the real one is to use the compressive response with duration of τ_0 as a "Pseudo" force function. As an example, the comparison is made between frequency spectrum of the original half-sine force function and that of the pseudo force for the case of τ_D equal 2, as shown in Figure 9. For this specific case of τ_D, the pseudo force spectrum agrees well with the real force spectrum since τ_0 is close to τ_D. As τ_0 becomes much smaller than τ_D, it can be expected that the difference between the two spectra would be more significant. In addition, the first zero of the frequency spectrum for the half-sine force is at frequency $1.5/\tau_D$.

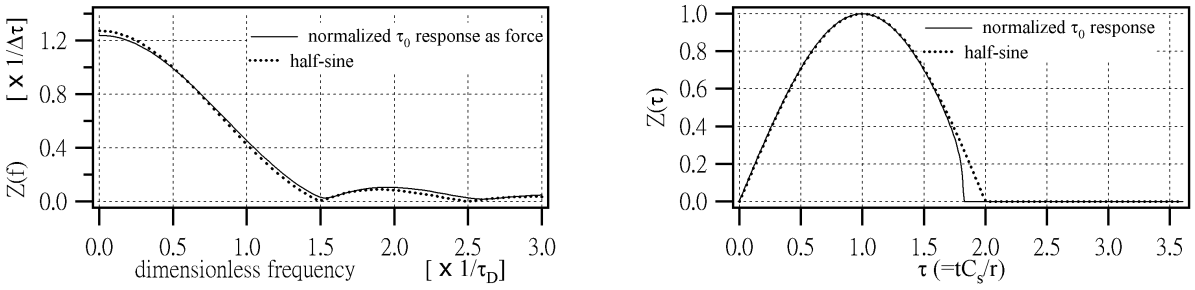

(a) frequency spectra

(b) force-time function

Figure 9. Frequency spectra associated with half-sine force for $\tau_D = 2$

Similar behavior can be observed from responses due to other force functions, as shown in Figure 10. When comparing between the real spectra (dashed curves) shown in Figures 9 and 10, it is clear that the ordinate of the half-sine curve at zero frequency is the highest and the frequency of the first near-zero amplitude for the other curves extend to frequencies higher than $1.5/\tau_D$. Owing to their smaller durations, the pseudo curves (solid curves) are always smoother than the real curves (dashed curves), in which the formers have lower ordinates at zero frequency and also higher frequencies for the first zero or near-zero amplitude. Such effects may be compensated one way or another by changing the force function to a half-sine function since the half-sine function results in relatively steepening effect among the various force functions. This means that, when replacing the real forces with the half-sine force and a duration smaller than τ_D, the equivalent spectrum may be similar to the real one. In Figure 10, the marked curves represent the equivalent spectra computed by a half-sine function with duration τ_0. Except for the triangle force, the equivalent spectra appear better than or at least as good as the pseudo

ones in matching the real spectra. The trough-to-ending duration τ_d is always larger than the compressive duration τ_0 and thus the equivalent spectrum using duration of τ_d would be steeper than the τ_0 one. In several cases, the equivalent half-sine τ_0 spectra agree well with the real ones in Figure 10. Since, for cases where τ_0 almost equals to τ_D, the over-estimate by the half-sine force cannot be balanced. The equivalent half-sine τ_0 spectra become much steeper than the real spectra for cases of very large values of τ_D. As a result, the use of an equivalent half-sine spectrum with a duration of τ_0 can potentially provide good approximations for the real spectrum, providing the value of τ_D is relatively large.

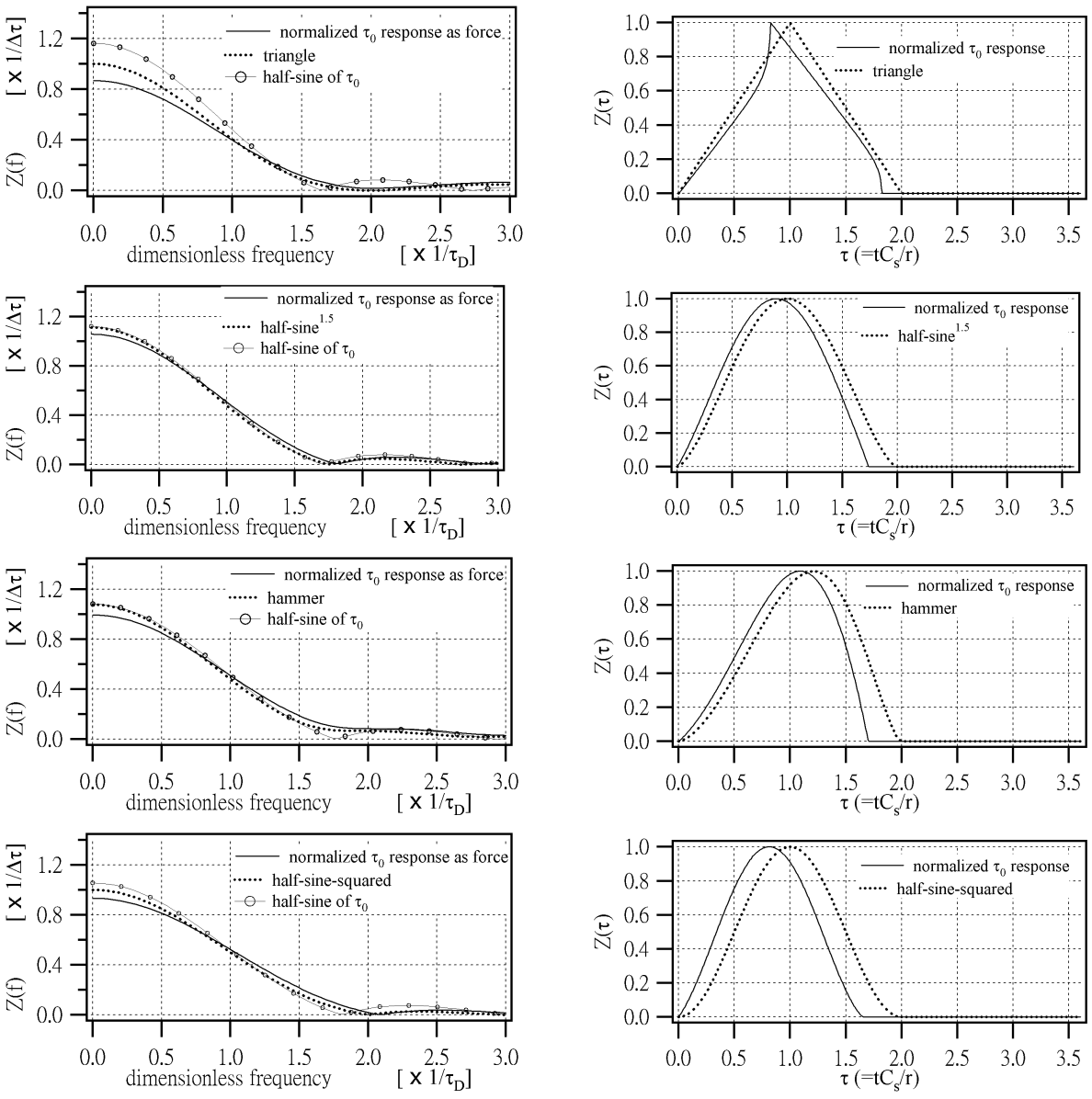

(a) frequency spectra (b) force-time function

Figure 10. Frequency spectra associated with various force functions for $\tau_D = 2$

The spectra associated with a small impact duration is shown in Figure 11, in which the half-sine-squared force has an impact duration τ_D equals 0.2. The differences among τ_d, τ_0 and τ_D are more significant for smaller values of τ_D, as mentioned in the pervious section. It can be seen that both the pseudo spectrum computed directly from the compressive response of duration τ_0 and the equivalent half-sine spectrum with τ_0 become much less steeper than the real spectrum. The equivalent half-sine spectrum obtained with duration τ_d appears to be steeper than the real spectra. As can be expected, both equivalent spectra are steeper than the pseudo spectrum. A smoother curve has smaller amplitude within the lower frequency region and larger amplitude within the higher frequency region. When the frequency associated with the point of intersection between a smoother curve and a steeped curve is defined as "trend-reverse" frequency, the trend-reverse frequency seems to be about half of the frequency of the first near-zero amplitude, in the range between $0.75/\tau_D$ and $1/\tau_D$. Apparently, the equivalent half-sine spectra with τ_d and τ_0 may serve as the upper and lower bounds of the real spectrum. Another example is shown in Figure 12, where the equivalent half-sine spectra for the half-$\sin^{1.5}$ force is plotted for $\tau_D = 0.2$. The τ_0 curve approaches closely to the lowered pseudo spectrum while the τ_d curve appears to be still higher than the real spectrum. As τ_D decreases the half-sine τ_0 curve moves towards the pseudo spectrum, and the half-sine τ_d curve is steeper than but approaches downward to the real spectrum.

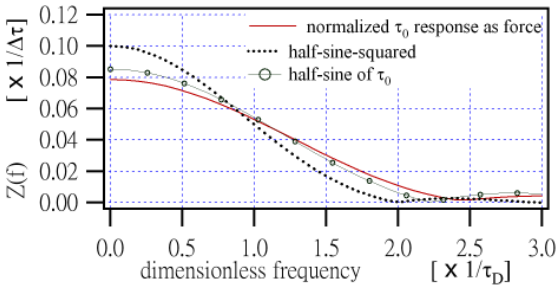

(a) frequency spectra (marker represents half-sine τ_0)

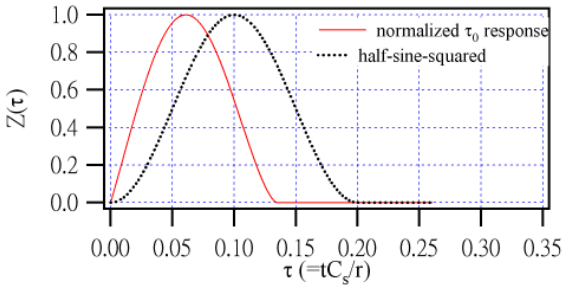

(b) force-time function

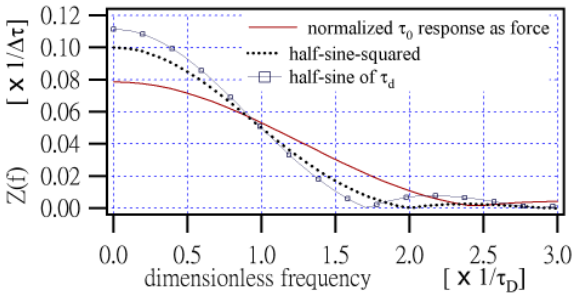

(c) frequency spectra (marker represents half-sine τ_d)

Figure 11. Frequency spectra associated with half-sine-squared force for $\tau_D = 0.2$

Based on the above findings, we can conclude that, when τ_D is large, the real spectrum would fall between the equivalent half-sine spectrum of τ_0 and the pseudo spectrum defined by the compressive duration τ_0. The former could be steeper while the latter is slightly smoother than the real spectrum. On the other hand, for very small τ_D, the equivalent spectrum of τ_d seems to be the closest one of all to the real spectrum. For moderate values of τ_D, the real spectrum obviously locates somewhere between the two equivalent half-sine spectra. To illustrate this point, we arbitrarily assume that the duration τ used in computing the equivalent half-sine spectrum linearly varies with the amplitude ratio (A_t/A_{peak}). The amplitude ratio is within zero and the maximum ratio listed in the bottom row of Table 3. The equivalent half-sine spectrum with a duration τ linearly interpolated between τ_0 and τ_d is shown in Figure 12(d). As can be expected, this equivalent spectrum is somewhat better than the half-sine τ_d curve in matching the real spectrum.

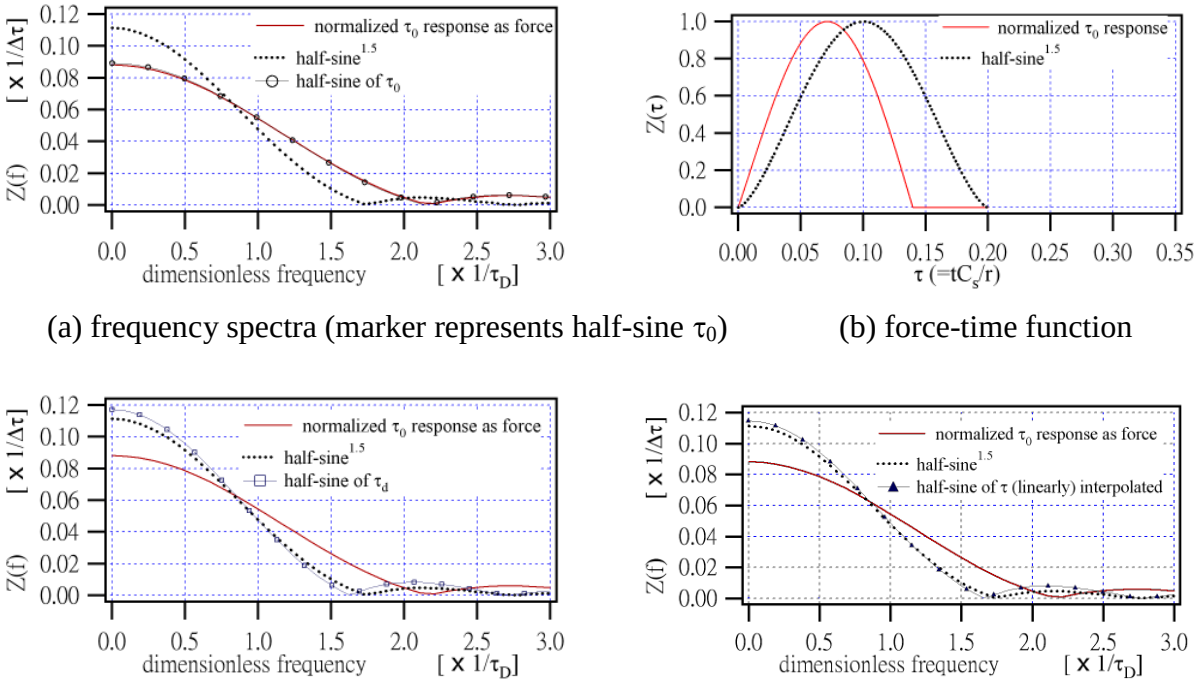

(a) frequency spectra (marker represents half-sine τ_0) (b) force-time function

(c) frequency spectra (marker represents half-sine τ_d) (d) interpolated curve

Figure 12. Frequency spectra associated with half-sin$^{1.5}$ force for τ_D = 0.2

The second example of such interpolated spectrum where a moderate τ_D of 1 is selected is shown in Figure 13. From Table 3, we recognize that (A_t/A_{peak}) ratio is 0.234 and the extreme ratios associated with $\tau = \tau_0$ and $\tau = \tau_d$ are 0 and 0.62, respectively. From Table 5, the corresponding values for τ_0/τ_D and τ_d/τ_D are 0.807 and 0.948. The equivalent duration can be obtained from interpolating 0.234 between 0 and 0.62. Thus the resulting duration equals to $\tau = 0.86\tau_D$. Again, it is obvious that the interpolated spectrum agrees well with the real spectrum.

For practical Impact-Echo tests on concrete surface, the dimensionless impact duration τ for the near-source receiver (typically a radial distance of 3-cm) is normally higher than 2 and seldom less than 1. Thus, the only parameter we need to normalize an Impact-Echo spectrum is simply the compressive duration

τ_0. Neither τ_d nor the interpolation process is required in recovering a simulated transfer function associated with an impact test.

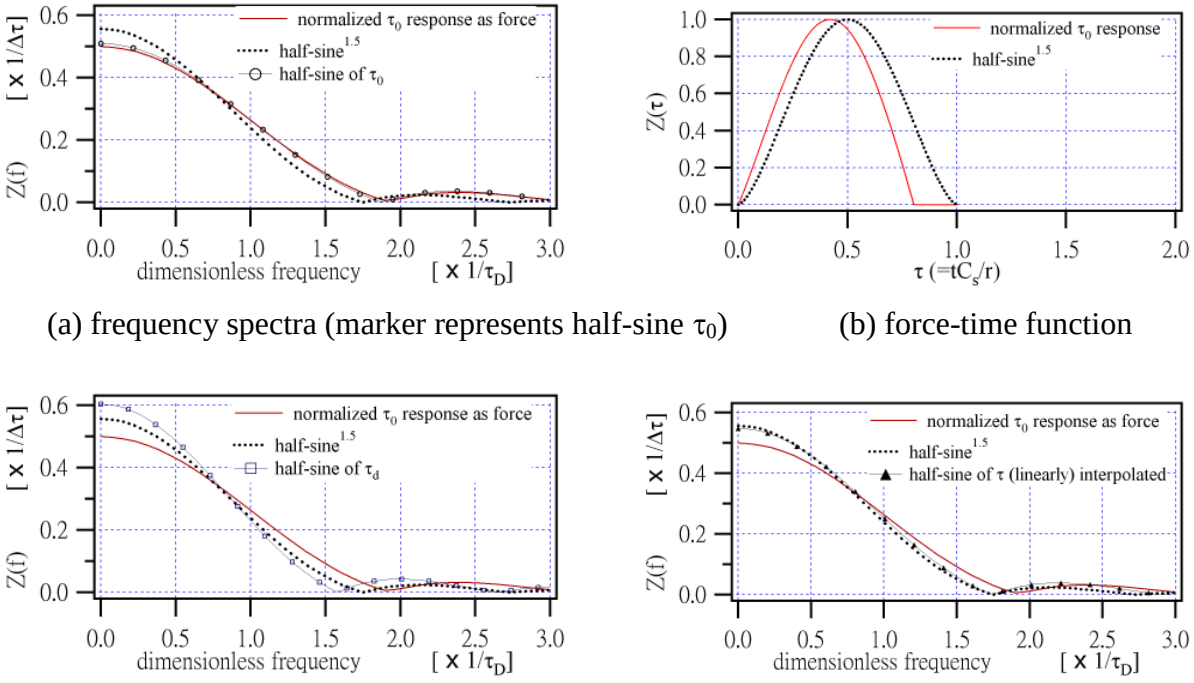

(a) frequency spectra (marker represents half-sine τ_0) (b) force-time function

(c) frequency spectra (marker represents half-sine τ_d) (d) interpolated curve

Figure 13. Frequency spectra associated with half-sin$^{1.5}$ force for τ_D = 1

Computation of simulated transfer function

Consider two normalized functions $f_u(t)$ and $W_u(t)$ with their maximum amplitudes equal to a unit amplitude. The force and response functions are expressed as $f(t)=Zf_u(t)$ and $W(t) = ZA_{peak}W_u(t)$, respectively. Since the amplitude of the equivalent force function is equal to that of W(t), that is ZA_{peak} or ZYA_0, the equivalent force function can be expressed as $f_e(t) = ZA_{peak}f_{ue}(t)$. $f_{ue}(t)$ is a pseudo force function, such as the half-sine function or the compressive response corresponding to $W_u(t)$, of unit amplitude. The transfer function can then be expressed in terms of the Fourier transform pairs of $f_u(t)$ and $W_u(t)$ as

$$\frac{\hat{W}(f)}{\hat{f}(f)} = \frac{ZA_{peak}\hat{W}_u(f)}{Z\hat{f}_u(f)} = A_{peak}\frac{\hat{W}_u(f)}{\hat{f}_u(f)} \cong A_{peak}\frac{\hat{W}_u(f)}{\hat{f}_{ue}(f)} = YA_0\frac{\hat{W}(f)}{\hat{f}_e(f)} \tag{9}$$

with

$$\hat{f}_e(f) = ZA_{peak}\hat{f}_{ue}(f) \cong ZA_{peak}\hat{f}_u(f)$$

Equation (9) indicates that the ordinate of transfer function is of the order of A_0 and thus depends on radial distance *r*, shear modulus G, and Poisson's ratio ν. Test data of approximately the same mass density and Poisson's ratio, as in the case for concrete specimens, can be compared based on the following conditions. Assume that *r* = 0.03m and C_p = 4000 m/s. A relatively long impact duration is also assumed such that Y = 1. The default transfer function can then be expressed as

$$\left[\frac{\widehat{\mathrm{W}}(f)}{\widehat{\mathrm{f}}(f)}\right]_{default} = \mathrm{A}_0(r, C_p)_{default}\left[\frac{\widehat{\mathrm{W}}_\mathrm{u}(f)}{\widehat{\mathrm{f}}_\mathrm{u}(f)}\right] = \mathrm{A}_0(0.03, 4000)\left[\frac{\widehat{\mathrm{W}}_\mathrm{u}(f)}{\widehat{\mathrm{f}}_\mathrm{u}(f)}\right] \tag{10}$$

with an ordinate constant $\mathrm{A}_0(0.03, 4000)$. A_0 is inversely proportional to r and the square of C_s (also C_p) as shown in Equations (2) and (3). A scaled transfer function can be obtained as

$$\left[\frac{\widehat{\mathrm{W}}(f)}{\widehat{\mathrm{f}}(f)}\right] \Big/ \mathrm{A}_0(r, C_p)_{default} = \mathrm{Y}\left(\frac{\mathrm{A}_0(r, C_p)}{\mathrm{A}_0(0.03, 4000)}\right)\left[\frac{\widehat{\mathrm{W}}_\mathrm{u}(f)}{\widehat{\mathrm{f}}_\mathrm{u}(f)}\right] = F_n\left[\frac{\widehat{\mathrm{W}}_\mathrm{u}(f)}{\widehat{\mathrm{f}}_\mathrm{u}(f)}\right] \cong F_n\left[\frac{\widehat{\mathrm{W}}(f)}{\widehat{\mathrm{f}}_\mathrm{e}(f)}\right] \tag{11}$$

where

$$F_n = \mathrm{Y} \times \left(\frac{4000}{C_p}\right)^2 \times \left(\frac{0.03}{r}\right)$$

Accordingly, we define a simulated transfer function which is computed from the surface response function W(t), the equivalent force function $\mathrm{f_e}(t)$, and a scale constant F_n.

The frequency counterpart of the equivalent force function $\mathrm{f_e}(t)$ can be obtained via computer programs using FFT algorithm. However, the amplitude of the Fourier transform for a unit half-sine function with duration $\mathrm{t_D}$ can be explicitly expressed as,

$$\left|\mathbf{F}(f)\right| = \left|2\cos(\pi t_D f)\frac{t_D}{\pi(1-4t_D^2 f^2)}\right| \tag{12}$$

with f representing the sampling frequency. The FFT computation can thus be omitted when deducing the equivalent half-sine spectra.

5. Experimental application

In this section, the application of the proposed approach to the quantification of Impact-Echo signals is illustrated with experimental data. Two examples are presented in which the first one contains impact tests at an identical location using three different impact sources, while the second case is associated with impact tests at different points on a uniform plate. It should be noted that the differences among thickness amplitudes resulted from repeated impacts for a specific steel ball are typically within 5% and could be as high as 10% for the smallest ball, the 3-mm ball. The test data shown in the first example are intentionally selected so that the thickness amplitudes recovered using pseudo forces for the three different steel balls can be almost identical. In the second example, six impact tests were performed at each location with a specific steel ball. The curves shown in figures are those corresponding to the test sets which give the intermediate value among the six impacts.

Example 1 :

In this example, a 60-cm×60-cm concrete plate specimen with 15-cm thickness is prepared and repeatedly tested at a pair of fixed points with steel balls of different diameters. The distance between the impact point and the near-source receiver is 3 cm. The P-wave velocity calculated from the first arrivals of the surface response histories at two receivers is 3970 m/s. The diameters of balls are 3, 5, and 6 mm and their corresponding compressive durations are 16, 29 and 36 μs, which are equivalent to τ_0 of about 1.38, 2.52, and 3.10, respectively. The recorded time histories of the impact responses and their frequency amplitude spectra are shown in Figure 14. It is apparent that both time and frequency responses associated with three different balls are very similar in terms of the major wave form and of the frequency contents near the thickness frequency. Since the frequency amplitude is a direct function of force amplitude and duration, the ordinates at the thickness frequency for different impacts are clearly

different from each other.

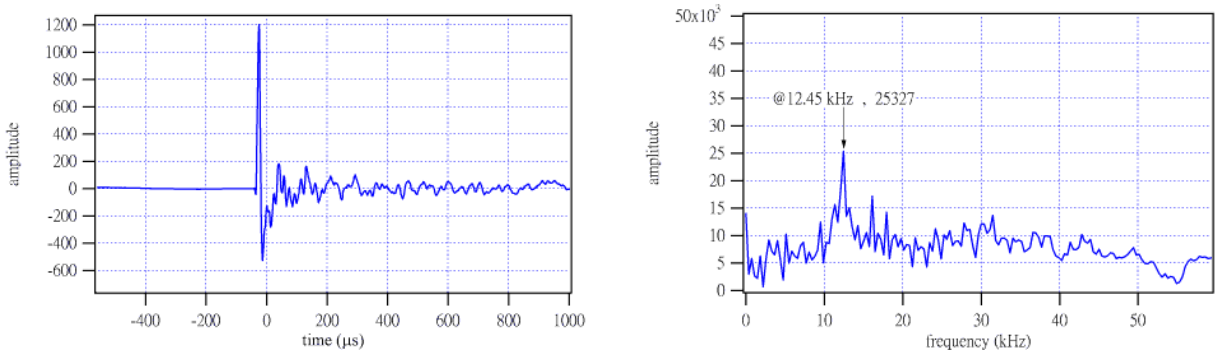

(a) 3-mm steel ball and 16-μs duration (τ_0 = 1.38)

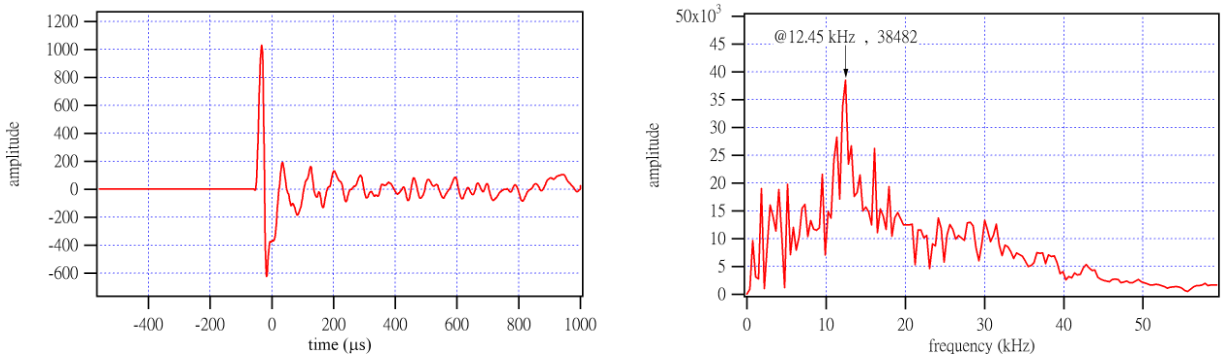

(b) 5-mm steel ball and 29-μs duration (τ_0 = 2.52)

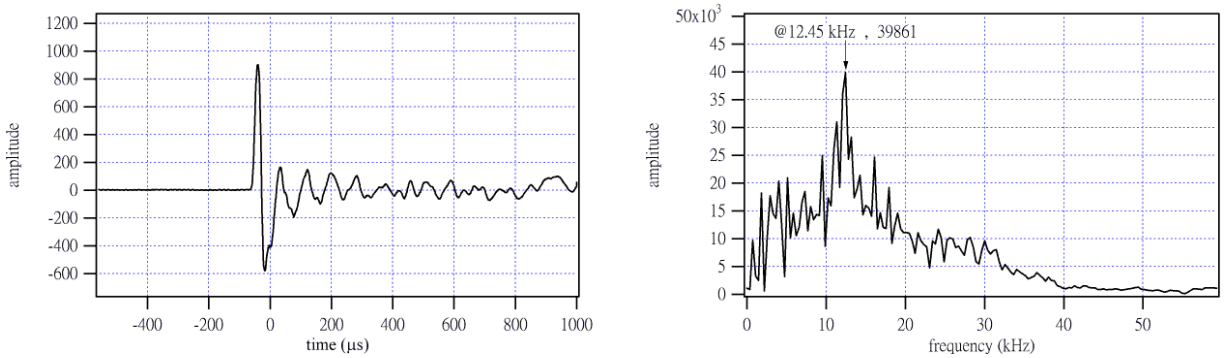

(c) 6-mm steel ball and 36-μs duration (τ_0 = 3.1)

Figure 14. Response wave forms and amplitude spectra with respect to three different impact steel balls (impacting at an identical point)

To illustrate the effect of using the half-sine amplitude curve in Figure 6 to generate simulated transfer functions, the three amplitude spectra in Figure 14 are normalized with respect to the pseudo impulses as shown in Figure 15. The scaled thickness amplitudes associated with all three impact sources appear to be very consistent. Although, what we illustrate in the Figures are selected to have very close scaled thickness amplitudes, these promising experimental data can be easily achieved and also be expected since all three curves are obtained by impacting at an identical point. The values shown in parentheses, on the other hand, represent the scaled thickness amplitudes which are calculated using half-sine impulses with duration τ_0. The differences among values in the parentheses are less than 4%. The trend-reverse frequencies associated with the three impact tests can be estimated by $0.75/t_0$ and are about 47, 26 and 21 kHz, respectively. Since the thickness frequency, 12.45 kHz, is much lower than the trend-reverse frequencies, the thickness amplitudes recovered by the half-sine force are clearly lower than those obtained with pseudo forces as can be expected. The recovered thickness amplitudes basically remain constant for different sizes of steel balls regardless of the (pseudo or equivalent half-sine) forces used. Figure 16 shows the force-time functions associated with the pseudo forces and the equivalent half-sine forces. It is obvious that, as impact duration becomes larger, the skewness of the curves becomes more significant.

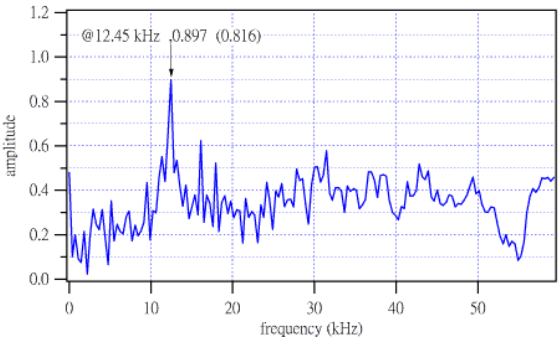

(a) 3-mm steel ball and 16-μs duration

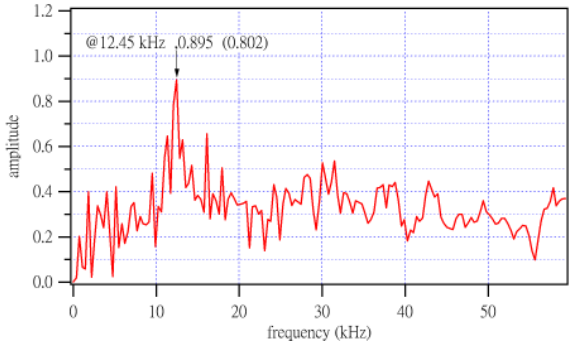

(b) 5-mm steel ball and 29-μs duration

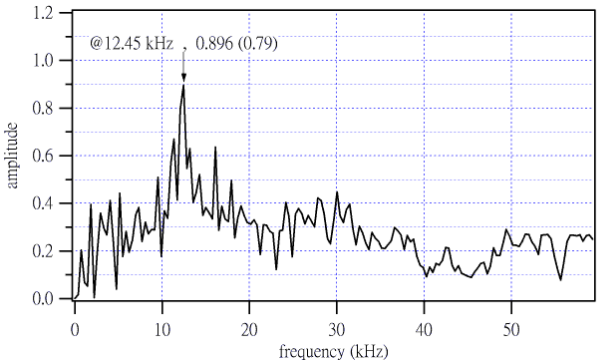

(c) 6-mm steel ball and 36-μs duration

Figure 15. Simulated transfer functions with respect to three different impact steel balls

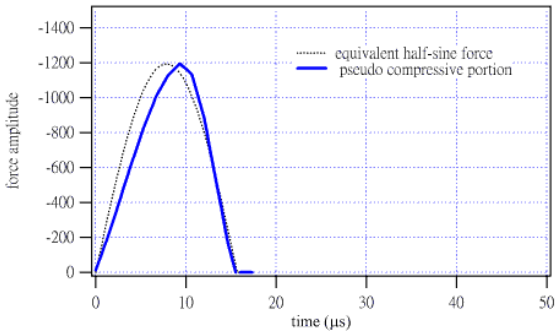

(a) 3-mm steel ball and 16-μs duration.

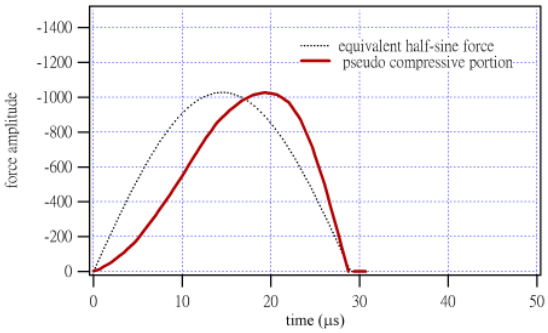

(b) 5-mm steel ball and 29-μs duration

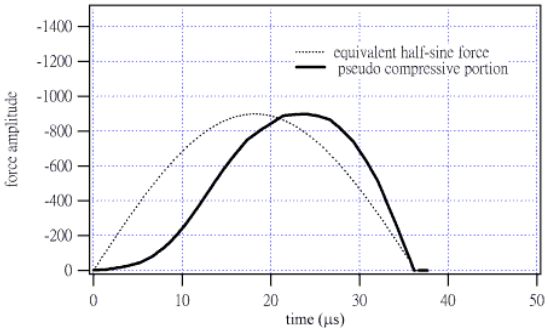

(c) 6-mm steel ball and 36-μs duration

Figure 16. Simulated force-time functions with respect to three different impact steel balls

Example 2 :

In the second example, impact tests are performed on an 80-cm×80-cm concrete plate specimen with a thinner thickness, 9-cm. Three sizes of balls, 3-mm, 5-mm and 6-mm in diameters, are used as impact sources at three different points, specified as A, B, and C. The distance between the impact point and the receiver is kept 3 cm. The P-wave velocity recovered from the first arrivals of the surface response histories at two receivers is about 3750 m/s. The corresponding compressive duration t_0 are about 15, 36 and 41 μs (τ_0 = 1.19, 2.93, 3.34), respectively. The estimated trend-reverse frequencies ($0.75/\tau_0$) of the force spectra are around 51, 21 and 18 kHz.

It is shown in Figure 17 the time histories and frequency amplitudes of the surface displacement responses for three specific test sets. Comparing to what we saw in the previous example, the differences in both wave forms and frequency amplitudes of the three impact tests are more obvious since they are recorded at different locations. The thickness frequency amplitude for the 5-mm steel ball are about 85% and 50% higher than those of the 3-mm and 6-mm steel balls. After scaling the frequency spectra with the proposed pseudo force spectra, the simulated transfer functions of the three impact tests provide consistent values for amplitudes at the thickness frequency. The differences among thickness amplitudes are less than 5%, as shown in Figure 18. The values in parentheses stand for the frequency amplitudes obtained using the half-sine approach. Note that the amplitude of the 3-mm (15μs) is smaller than those of the 5-mm (36μs) and the 6-mm (41μs). The near identical amplitudes in Figures 18(b) and 18(c) are due to the fact that corresponding force spectra have almost the same ordinate near

the trend-reverse frequency.

What worth of mentioning is that the thickness amplitude caused by the real force might be very close to the constant value shown in Figure 18(b) or 18(c) since the force-frequency amplitude of the real force could be close to the estimated ones near the trend-reverse frequency. The differences among these three values obtained from the half-sine approach are around 7% which is slightly larger than that of the pseudo approach, 4%. Moreover, the thickness frequencies 20.5 kHz and 19.77 kHz indicate that the recovered thicknesses of the plate, 8.8 cm and 9.1 cm, are close to the designated 9-cm. Consequently, the two proposed procedures can both provide reasonably consistent thickness amplitudes in the simulated transfer function, even when surface responses are generated using different impact sources at different locations on the plate surface.

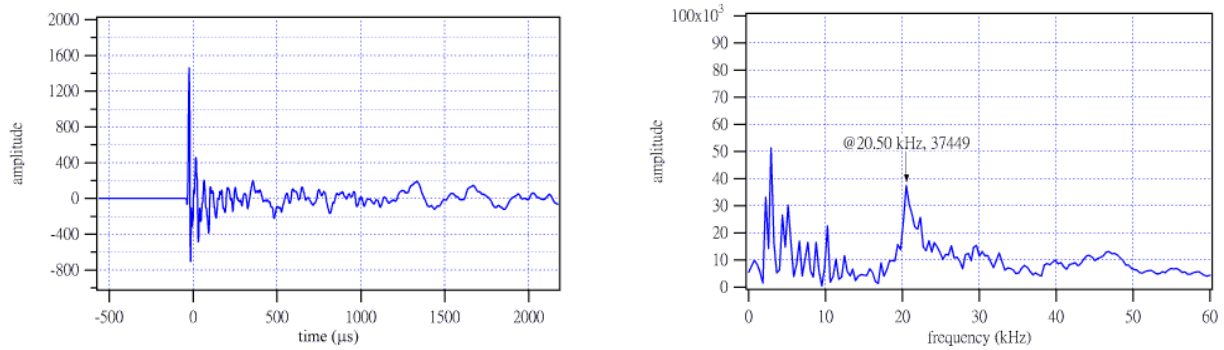

(a) impact responses at point A using 3-mm steel ball (15-μs duration)

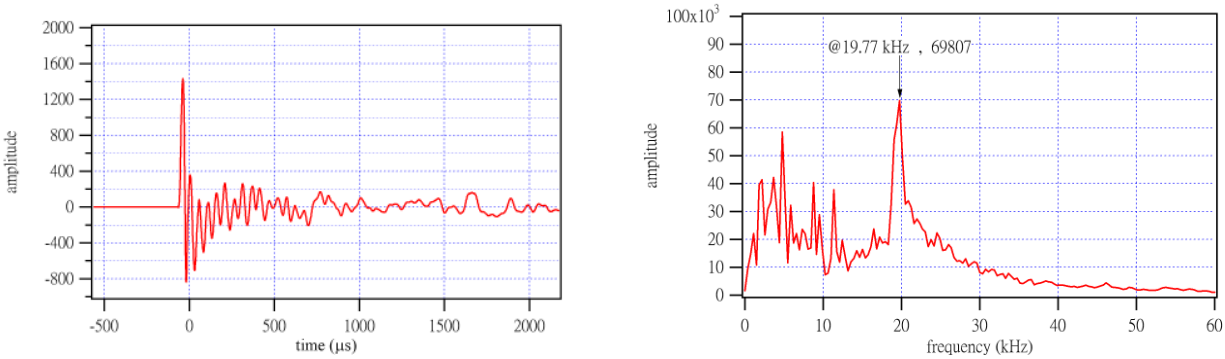

(b) impact responses at point B using 5-mm steel ball (36-μs duration)

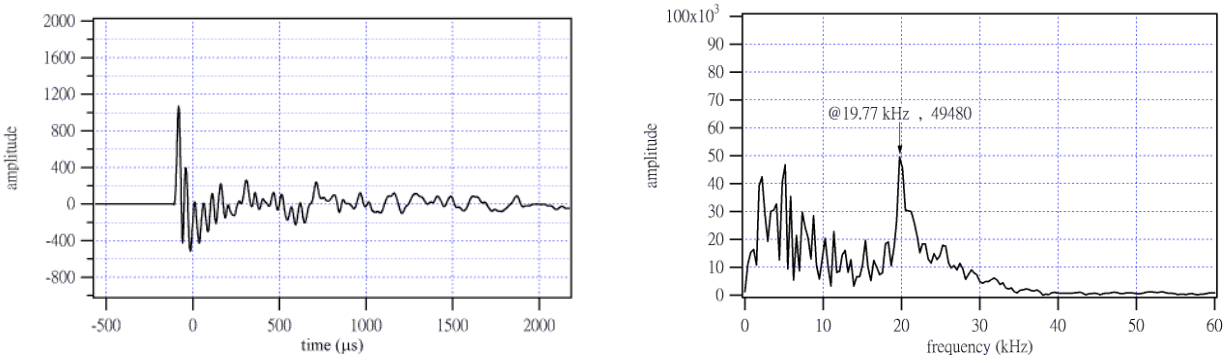

(c) impact responses at point C using 6-mm steel ball (41-μs duration)

Figure 17. Surface displacement responses by impacting three steel balls at different locations

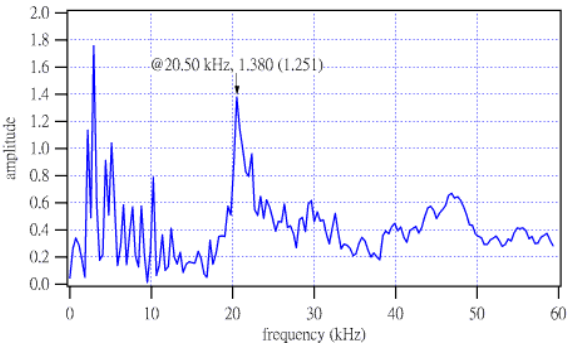

(a) 3-mm steel ball (15-μs duration) at A

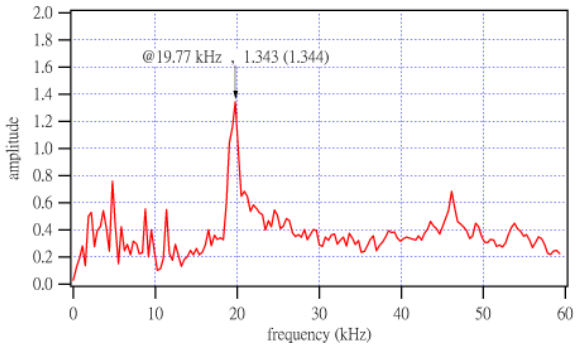

(b) 5-mm steel ball (36-μs duration) at B

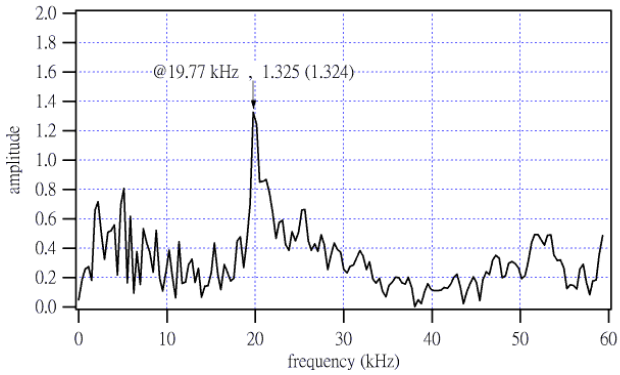

(c) 6-mm steel ball with 41-μs duration at C

Figure 18. Simulated transfer functions of the three impacts corresponding to Figure 17

6. Conclusions

The analytical solution for the normal surface displacement due to the Heaviside force has been reviewed and applied to compute the surface responses caused by various impulse-type force functions. A series of numerical studies on the direct Rayleigh response are carried out to analyze the variations of the response amplitudes and the response durations associated with the direct wave form. Based on the varying trends constructed by half-sine-powered forces, it can be concluded that the simple half-sine function with duration τ_0 provides frequency contents similar to those of the designated force functions. Accordingly, an equivalent force function can be easily established with amplitude curves that are numerically obtained using half-sine function as the impact force. In order to make comparison between different impact responses, a simulated transfer function is proposed, as Equation (11). Amplitudes at the thickness frequency can now be properly scaled and also remain constant for a uniform specimen.

In computing the normal surface displacement, numerical results are obtained by superposing responses calculated based on the analytical solution associated with the Heaviside step force. The well-known Pekeris' explicit solution for Poisson's ratio of 0.25 is extended to a more general expression which is valid for Poisson's ratio of arbitrary values. Such explicit formulation may potentially be useful to the investigation on related research topics.

For the construction of relationship between

response amplitude and force duration, various force functions all lead to similar trends. These trends can be separated into three regions such that approximations can be made by three simple mathematic expressions, as shown in Equation (8). For a given radial distance r, relatively small durations result in attenuation of amplitude of $r^{-0.5}$, while relatively long durations cause amplitudes attenuated with r^{-1}.

Because the value of a transfer function is dependent on radial distance, shear modulus, and Poisson's ratio, a scaled transfer function is proposed as shown in Equation (11). The scale factor in Equation (11) is the ordinate constant of the transfer function associated with a designated test situation where radial distance is 0.03 m, P-wave velocity is 4000 m/s, and impact duration is relatively large. Such factor is equivalent to the nominal amplitude factor A_0 defined in Equation (3) and can be arbitrarily adjusted according to the attribute of tests. The advantage of using a scaled transfer function is that the ordinate of thickness amplitude can be of the order near unity. Thus, it provides more manifest intuition than that of the real transfer function.

The realistic impact is usually highly field-sensitive and the compressive portion of surface response essentially retains the shape of the impact force. Using a pseudo force function is comparatively better than using the equivalent half-sine force in providing sTable values for the thickness amplitudes. However, the half-sine approach allows one to deduce transfer functions without the need of FFT computation. Thus, the half-sine approach is a relatively simpler alternative to calculate the normalized amplitude at the thickness frequency.

From the two application examples of Impact-Echo experiments, it is found that the proposed approach can recover steady values for the thickness amplitude not only for tests at a fixed location but also for tests using various impact sources at different locations. When thickness amplitudes obtained for an identical specimen remain constant regardless of the impact sources and locations, the thickness amplitude can serve as an index to evaluate the impedance change at the bottom interface of the specimen. The simulated transfer functions computed for two groups of experimental data demonstrate the capability of the proposed method in quantifying the thickness amplitude for Impact-Echo tests. The results show that the proposed approach is very promising and can be extended to evaluate the information of substrate layers.

Appendix: list of symbols

A_0 : permanent normal surface displacement due to Heaviside step force
A_{peak} : compressive peak amplitude of the direct Rayleigh waveform
A_t : trough amplitude of the direct Rayleigh wave form
a, b, c : roots of Rayleigh characteristic Equation $R(y^2) = 0$, c is the largest root
C_p , C_s , C_R : P, S, and Rayleigh wave velocities
$\mathbf{F}(f)$: Fourier transform of a unit half-sine function
F_n : scale constant of simulated transfer function
F : sampling frequency
$f(t)$: force-time function
$f_u(t)$: normalized function of f(t) with a unit amplitude
$f_{ue}(t)$: approximation function of f_u(t)
G : shear modulus
ρ : mass density
γ : ratio of S-wave velocity to Rayleigh wave velocity ($=\sqrt{c}$)
H(t) : Heaviside step function
μ : Lame's constant = G
ν : Poisson's ratio
$R(y)$: characteristic Equation of Rayleigh wave
R : radial distance
σ : ratio of S-wave velocity to P-wave velocity

t : elapsed time
t_0 : duration of compressive portion of the direct Rayleigh wave form
t_D : impact duration
t_d : trough-to-ending duration of the direct Rayleigh wave form
τ : dimensionless time parameter ($=C_s t/r$)
τ_0 : dimensionless compressive response duration ($=C_s t_0/r$)
τ_D : dimensionless impact duration ($=C_s t_D/r$)
τ_d : dimensionless trough-to-ending response duration ($=C_s t_d/r$)
$W(t)$: normal surface response due to force-time function
$W_u(t)$: normalized function of W(t) with a unit amplitude
$w(t)$: normal surface response due to the Heaviside step function
X : ratio of impact duration to the R-wave arrival time ($=\tau_D/\sqrt{c}$)
x , $\hat{x}$: Fourier transform pair
Y : ratio of A_{peak} to A_0
Y : dimensionless variable defined as C_s/C_R
Z : amplitude of the Heaviside step force

References

[1] Pekeris, C. L. 1955. The Seismic Surface Pulse, *National Academy of Science, U.S.A.*, 41: 629-638.

[2] Achenbach, J. D. 1973. *"Wave propagation in elastic solids"*, North-Holland, New York: 310-318.

[3] Graff, K. F. 1975. *"Wave motion in elastic solids*, Dover, Oxford: 356-368.

[4] Wu, T. T., Fang, J. S., Liu, G. Y., and Kuo, M. K. 1995. Determination of Elastic Constants of A Concrete Specimen Using Transient Elastic Waves, *Journal of Acoustic Society of America*, 98, 4: 2142-2148.

[5] Cheng, C. C., Yu, C. P., and Chang, H. C. 2004. On The Feasibility of Deriving Transfer Function from Rayleigh Wave in the Impact-Echo Displacement Waveform, *Key Engineering Materials*, 270-273: 1484-1492.